International Journal of Emerging Engineering and Technology (IJEET)
ISSN (e): 2958-3764
Volume: 5, Number: 1-2, Pages: 54 - 62, Year: 2026 (Special Issue)

Cellular IoT Based System for Dynamic Real-Time Pollution Mapping in Urban Environment

Pakeeza Noor, Sundus Ali, Irfan Ahmed and Muhammad Imran Aslam *

Department of Telecommunications Engineering, NED University of Engineering and Technology, Karachi, Pakistan
*Corresponding author: Muhammad Imran Aslam (Email: iaslam@neduet.edu.pk)

Received: 08/08/2026, Revised: 29/09/2026, Accepted: 10/10/2026

***Abstract*—Rapid urbanization in developing countries poses air pollution challenges for urban areas caused by industry and vehicle emissions. Challenges associated with traditional air pollution monitoring technologies include high costs and poor portability and geographic coverage, which make it difficult to monitor short-term and localized air pollution. Other low-cost IoT solutions relying on Wi-Fi or LoRaWAN technology have their own limitations for outdoor use and dependence on local infrastructure, which can make monitoring and other applications difficult in other developing parts of South Asia. This paper presents the design and testing of a low-cost, portable IoT system for monitoring and mapping short-term and localized air pollution. The system monitors several air pollutants, including temperature, humidity, CO, and CH_4, and includes GPS and a two-part communications system involving a GSM network for in-field data collection and Wi-Fi and the Firebase cloud platform for remote data reporting. The system hardware is designed in two-layer format to separate the power supply circuitry from the sensing system. A real-time web and mobile dashboard provide interactive spatial visualization of pollution hotspots. To demonstrate the usability of the developed system, field tests were conducted over a 14.2-kilometer urban route in Karachi, Pakistan, in the morning and night. Test results show positive GPS mapping and data collection at nine sample sites and differences in other measured parameters between morning and night samples. Applications of this technology include a infrastructure-independent complement which is scalable to fixed monitoring networks in other areas lacking monitoring capabilities and, with calibration using data from other monitors, detailed air quality studies to support smart city and public health projects.**

***Index Terms*—Air Quality, Cellular IoT, Data Visualization, GSM, Pollution Mapping, Urban**

I. Introduction

URBAN air pollution is particularly caused by unplanned urbanization, industrialization, number of increasing cars and the rapid expansion of urban areas. Air pollution is hence one of the most critical environmental threats worldwide. The health consequences of carbon monoxide (CO), methane (CH_4), nitrogen oxides and air pollution particles include cardiovascular and respiratory diseases and reduced life expectancy [1],[8]. The levels of pollution fluctuate significantly with distance and time in a densely populated area. Site-specific, real-time measurements of air pollution can be made with high precision monitoring stations sustained by environmental agencies, based on customary air quality monitoring. High installation and maintenance costs, in addition to the accuracy and compliance standards, limit the density of these networks and therefore their spatial coverage. Pollution hotspots caused by factories, traffic congestion or other point sources may remain unobserved [2]. Stationary stations are fixed; thus, they cannot capture variations in pollution levels that occur over seconds in urban areas. Novel developments in the Internet of things (IoT) have facilitated the development of cost effective mobile environmental sensors based on microcontrollers and embedded sensor [3]. IoT cloud-based solutions allow real time data viewing, remote monitoring, and continuous collection of data. On the other hand, many IoT air quality solutions depend on Wi-Fi or other short-range wireless links, which restricts their use in mobile and outdoor settings [4].

This research addresses several contributions, which include (i) first of all it proposes a two-layer hardware architecture in which transmitter node physically segregates the processing and sensing circuits from the electrical supply unit. This choice came from a practical requirement to reduce the impact of power supply system on the sensor circuitry during field deployment of mobile systems. Typically, earlier IoT-based air quality monitoring systems did not address this issue its benefit is discussed qualitatively and was not quantified in this study. (ii) secondly, it introduces a dual-channel for communication pipeline. First is field data collection through GSM the ensure 100% mobility in the cellular coverage region. Second is the cloud synchronization from central node through WiFi and Firebase [6]. This split adds robustness when one channel malfunctions. It also keeps the system working in different places without WiFi or LoRaWAN gateway infrastructure. (iii) The paper also demonstrates multivariate mobile monitoring which consist of both CO and CH_4 addressing data deficiencies in present mobile systems which mostly monitor particulate matter or CO_2 and leave the combustion-specific gases linked to vehicular and industrial emissions. (iv) lastly, the system was

This work is licensed under a Creative Commons AttributionShareAlike4.0 International License, which permits Unrestricted use, distribution, and reproduction in any medium, provided the original work is properly cited

evaluated in a live urban drive test under real-world traffic along a 14.2 km route in Karachi, Pakistan. The result is a proof-of-concept demonstration of GPS-tagged pollution mapping in a fast urbanizing South Asian city where specialized LPWAN infrastructure is not available.

The subsequent sections of this paper are structured as follows: section II synthesizes the design of system and methodology, section IV describes the development of system, section V discusses experimental findings, section VI presents the limitations of the study, and lastly section VII concludes the paper.

II. Related Work

Air quality measurement techniques include stationary monitoring systems and other low-cost and mobile IoT solutions [7]. Stationary monitoring systems use sophisticated equipment to measure air quality at a single location. Benefits and drawbacks of stationary monitoring systems include high cost and lack of portability and ability to measure air quality at multiple locations [7]. Compact sensors connected with economical microcontroller have led to the emergence of low-cost sensor nodes as an alternative [9]. Although these systems allow for more deployment at lower costs, they are often offline and immobile and do not provide remote monitoring to the user [10]. With the advent of affordable network services, researchers explored enabling the controlled connected with the sensors to upload sensor data on a cloud platform using IoT [11].

Wi-Fi has been one of the most widespread interfaces in indoor/campus IoT applications regarding air quality monitoring. Quoting [4], the authors considered Wi-Fi enabled IoT devices integrated with deep learning algorithms for occupancy based smart building automation, showing the effectiveness of employing the wireless technology in continuous sensing applications for environment control. Recent results in [13] show that the Authors presented a detailed analysis of available ESP32 architecture based low-power IoT devices, supporting their extensive use in indoor air quality monitoring applications. The research study in [14] presents an IoT based low cost indoor air quality monitoring system for dynamic public environments, yet another validation of the ESP32 class of devices for the targeted application. However, the very nature of Wi-Fi enabled devices relies on the presence of an access point infrastructure, limiting the application to indoor environments or urban areas with high WiFi coverage.

The LPWAN low power wide area network, in particular LoRa and LoRaWAN, have received significant research interest which is for outdoor air quality monitoring due to their long range communication capability and also it consumes low energy. The authors of [5] characterized an LPWA-based air quality monitoring implementation. Nevertheless, the authors in [15] have investigated augmenting a low cost LoRaWAN connected sensors node with machine learning based characterization that yields better CO, NO_2 and PM_2 readings accuracies under field deployment conditions. Jabbar et al. [16] also demonstrated verification of a LoRaWAN based IoT architecture for long range outdoor AQ monitoring showing dependable cloud synchronization of geographically nodes through the Things Network (TTN). In recent years still the research group in [17] prototyped a LoRaWAN based mobile AQ monitoring system for implementation in public health applications. However, LoRaWAN requires prior deployment of specialized gateway infrastructure [16], [18], which may not be available in many South Asian cities.

GSM based systems are ideally portable and suitable for outdoor applications of mobile. They enable long range transfer of monitored data points without reliance on localized internet based services Although GSM-integrated pollution monitoring systems have been deployed in urban areas, they generally lack real-time cloud connectivity or spatial visualization. Moreover, existing GSM based execution transmit data directly over limited use GPRS networks. This present constraints with consistency and prohibitive costs in areas with poor cellular service, which can be a concern in parts of expanding South Asian metropolitan areas, including Karachi. Hybrid two-layer communication architectures employing GSM based data synchronization and visualization have also not been well studied. With most of the implementations opting to utilize communication as a one channel data pipeline. This work aims to fill these disparities by presenting a novel multiparameter, GSM enabled, GPS tagged mobile monitoring system with the hybrid two-layer communication architecture, which is tested with the urban drive tests in Karachi, Pakistan.

Table I proposes a systematic comparison of illustrative IoT based air quality monitoring system. literature, ourselves included. Highlighted columns include communication technology used, measured metrics, stationary mobile deployment type, GPS geo-tagging ability, cloud visualization backend ability, and main constraint. This system utilizes a two-tier GSM and WiFi based communication protocol, mobile/outdoor deployment with GPS geo-tagging, and ability to sense multiple gases like CO and CH_4 which is rare in mobile IoT deployments.

III. METHODOLOGY FOR SYSTEM DESIGN

This section describes the design of the proposed portable, IoT-based air quality monitoring system for geo-tagged, real-time environmental observation, including the integration of its components and the flow of data from the sensors to the cloud. As shown in Fig. 1, the system has four main components: sensors, a mobile application, a gateway, and a cloud-based data storage and visualization platform. Fig. 2 explains the installation and use of the system, including wireless communication and cloud data storage and visualization. Four types of data can be collected by the sensor array: ambient temperature and humidity, measured with a DHT22 sensor [23]; CO concentration, measured with a ZE07-CO sensor [24]; and CH_4 concentration, measured with a TGS2611 semiconductor sensor [25].

TABLE I
Comparative Analysis of Existing IoT-Based AQMS Works

Ref.	Technology	Parameters Monitored	Deployment Type	GPS Tagged	Cloud / Visualization	Key Limitation
[5]	LoRaWAN / LPWAN	CO, NO_2, PM, Temp, Hum	Static	No	ThingSpeak	No GPS, no real-time mapping
[12]	Wi-Fi	CO, NO_2, $PM_{2.5}$, Temp, Hum	Static (Indoor)	No	Cloud dashboard	Wi-Fi only, indoor scope
[15]	LoRaWAN	CO, NO_2, $PM_{2.5}$	Static	No	TTN + ThingSpeak	No GPS, ML calibration complex
[19]	Wi-Fi / MQTT	CO_2, $PM_{2.5}$, Temp, Hum	Static (Indoor)	No	Cloud + predictive ML	Wi-Fi dependent, indoor only
[16]	LoRaWAN	NO_2, SO_2, CO_2, CO, $PM_{2.5}$	Static (Outdoor)	No	TTN + ThingSpeak + Virtuino	Requires LoRa gateway infra
[13]	Wi-Fi / Bluetooth Low Energy	Multi-parameter (general IoT)	Static	No	Cloud (general)	No gas sensing, no mobility
[20]	Wi-Fi	PM, VOC, CO_2, Temp, Hum	Static (Indoor)	No	Smart home dashboard	Indoor, no outdoor/mobile deployment
[14]	Wi-Fi	CO_2, PM, Temp, Hum, VOC	Static (Indoor)	No	Cloud dashboard	Wi-Fi dependent, no outdoor use
[21]	Wi-Fi	PM, CO, NO_x, Temp, Hum	Static (Industrial)	No	Firebase + AI forecasting	Industrial only, not mobile
[17]	LoRaWAN	$PM_{2.5}$, CO_2, Temp, Hum	Mobile	No	Cloud + Maps	Requires LoRa gateway infrastructure
[22]	GSM (Cellular IoT)	CO_2, $PM_{2.5}$, PM_{10}, Temp, Hum	Mobile	Yes	Dashboard + Google Maps	No CH_4/CO sensing, single comm layer
Proposed	**GSM + Wi-Fi (Dual) Dual-layer design mitigates single-channel failure**	**CO, CH_4, Temp, Hum**	**Mobile (Urban)**	**Yes**	**Firebase + Dashboard + Maps**	SMS dependent; gas channels uncalibrated

The sensors are connected to an Arduino UNO microcontroller on the mobile transmitter node, which also hosts a NEO-6M GPS module [29] and a SIM900A/SIM800L GSM module [27], [28]; the receiver (gateway) node is based on an ESP32 [26]. At start-up, the Arduino initializes the attached sensors and modules and checks the interface of the peripherals before it begins data acquisition. A battery-powered power supply allows for portability away from a permanent power source and the GPS module supplies ongoing latitude, longitude and time data to record temporal and spatial context of the measurements. Within the loop, the temperature, humidity, CO and CH_4 readings are sampled at regular intervals and converted to engineering units by the linear scaling described in Section IV-C. This scaling is a first-order conversion that does not compensate for temperature and humidity dependence or for cross-sensitivity (see Section VI). The converted values, together with the GPS coordinates and time stamp, are formatted as a data packet (Temp, Hum, CO, CH_4, Lat, Long, Time) and sent as an SMS through the GSM module to the receiver node, which acts as the intermediary between the field unit and the cloud backend. Because the uplink uses the cellular network, the field unit needs no Wi-Fi or LoRa gateway along its route, and several transmitter nodes could, in principle, report to the same receiver.

At the gateway, the ESP32 parses each incoming SMS and forwards the values over its onboard Wi-Fi to the Google Firebase Realtime Database [6], which stores each packet with an associated time stamp. The stored data feed the user interfaces. A Map view shows real-time pollutant concentrations at monitoring locations to help users see geographic patterns and track trends in air quality along a travel route over time. Dashboard view shows real-time and historical information on other topics related to devices and other conditions being monitored. Additional monitoring program functions are available in both views. After each transmission, processing, ingestion and logging cycle, the system returns to the start of the monitoring loop and continues to operate autonomously.

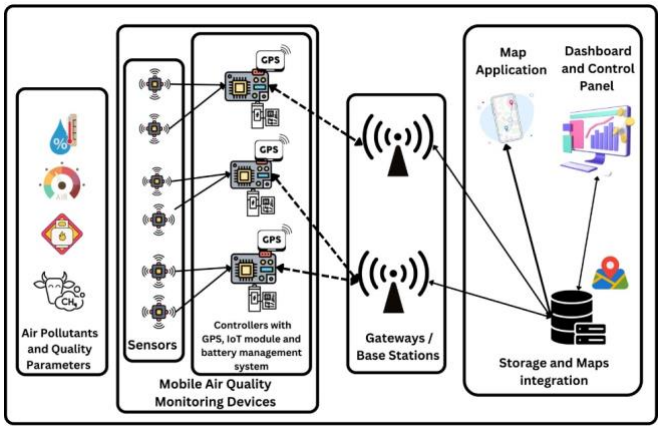


Fig. 1. Conceptual System showing end-to-end working of a cellular IoT AQMS

IV. System Development

A transmitter node and a receiver and cloud integration node make up the dual-module design of the developed system. After initializing all sensors and communication modules, the system gathers GPS and environmental data in real time. Before being

prepared and sent via GSM to a cloud platform, measurements are converted to engineering units by software scaling. A cellular IoT framework allows for continuous monitoring by time-stamped, storing, and visualizing data through dashboards and maps.

The system gathers temperature, humidity, gas levels, GPS positions, and timestamps after initializing sensors and communication modules, as seen in Fig. 3. Data is prepared as shown in Fig. 4 then transmitted to receiver node and then transmitted to Firebase via GSM following scaling and processing. It is saved, examined, and shown via dashboards and maps on the cloud. Continuous cellular IoT monitoring is repeated in the cycle.

A. Gateway Node Development

An ESP32 microcontroller interfaced with a SIM800L GSM module makes up the receiving node as shown in Fig. 5. Sensor values and GPS locations are taken from SMS messages by parsing them. The ESP32 connects to a network time protocol (NTP) server to make sure the time is correct and uses Wi-Fi to send organized JSON data to a Firebase Realtime Database. Cloud dashboards are used to show the data that is stored. These dashboards help with GPS-based pollution mapping. They also help with analysis and real time monitoring.

B. Sensor Node Development

The Arduino UNO microcontroller that powers the sensor node is interfaced with a number of sensors as shown in Fig. 6, including a TGS2611 sensor for methane detection, a ZE07-CO sensor for carbon monoxide detection, and a DHT22 sensor for temperature and humidity. Latitude and longitude data are provided in real time using a NEO-6M GPS [29] module. Periodically, GPS coordinates and sensor measurements are gathered and compressed into data packets. A SIM900A/SIM800L GSM module is used for data transfer, sending the sensor data via SMS at predetermined intervals.

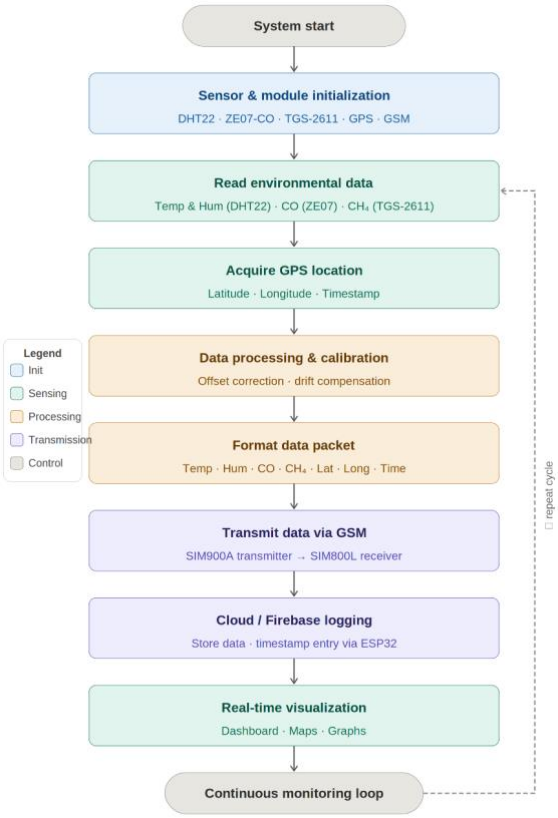


Fig. 2. The system working methodology

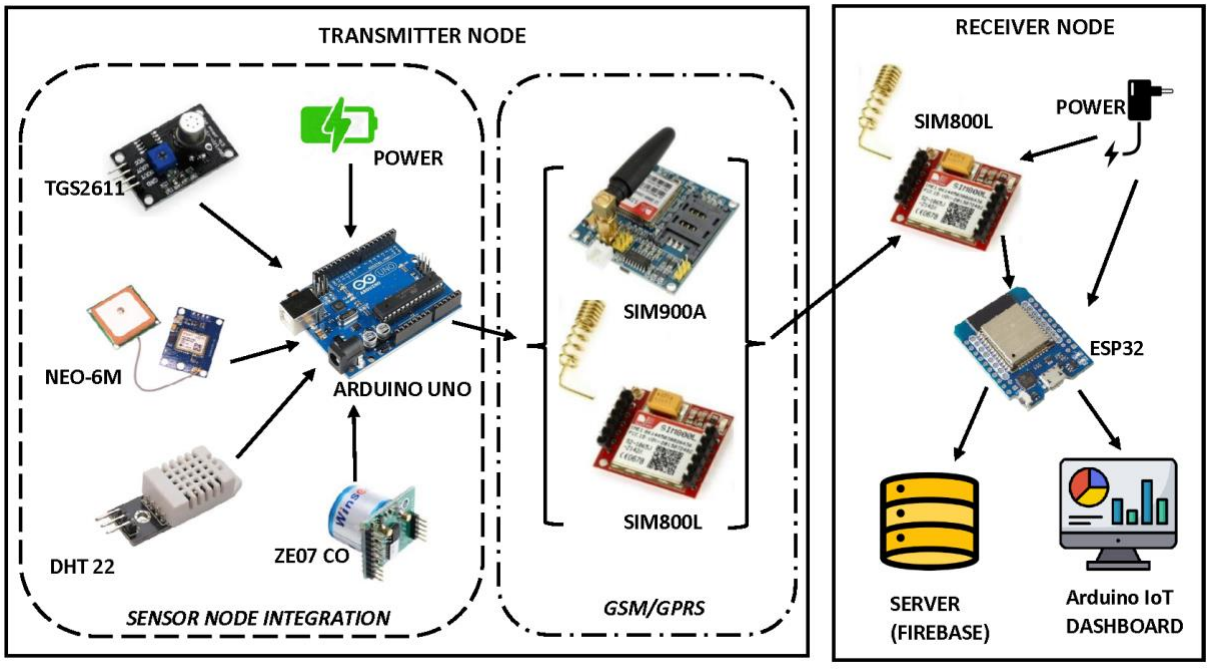


Fig. 3. System Functional Diagram

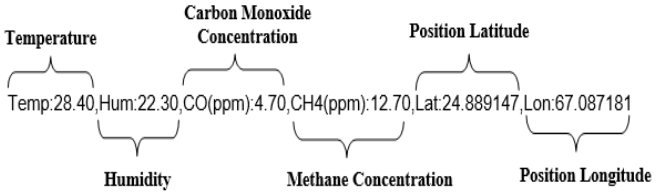


Fig. 4. Sample of SMS containing the data transmitted from sensor node to the gateway using GSM module.

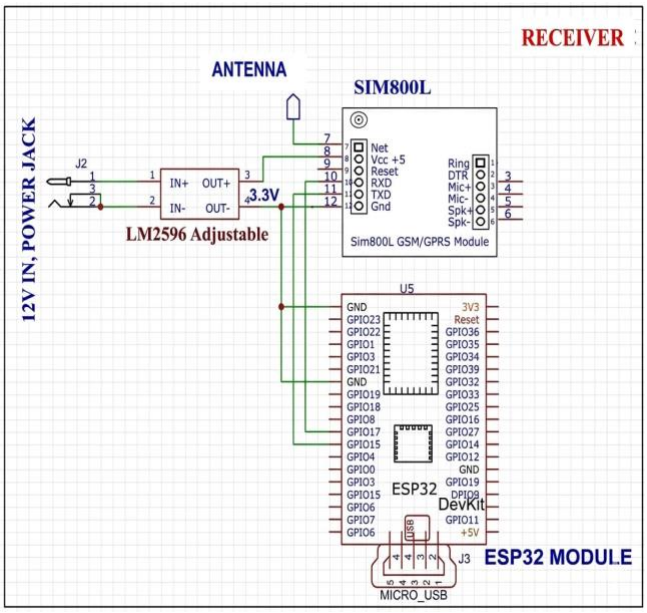


Fig. 5. Schematic configuration of the receiver node

C. *Sensors' Calibration*

The calibration of sensors in the system under development is done through linear software scaling, which transforms raw sensor signals into engineering units corresponding to the measured quantity. The DHT22 sensor provides calibrated (from manufacturer) values of temperature and humidity in digital form; thus, no calibration equations are needed. No comparison with co-located reference instruments was made in this study. The temperature and humidity uncertainty is therefore taken from the DHT22 datasheet (±0.5 °C and ±2% RH, up to ±5% RH) [23], and the gas channels are treated as uncalibrated indicators (see Section VI). the gas channels are considered to be uncalibrated indicators (see Section VI). For the purpose of gas sensing, calibration is done by converting analog-to-digital converter (ADC) values to voltages, and then linearly converting into gas concentration values. The ZE07-CO and TGS2611 sensors are connected to the Arduino's analog inputs, and their ADC outputs, in their raw form, are converted to voltage using the following formula:

$$V_{\text{out}} = \text{ADC} \times \left(\frac{5.0}{1023}\right) \quad (1)$$

Where ADC is the 10-bit reading (0–1023) of the Arduino analog input and 5.0 V is the ADC reference voltage, so that one ADC count corresponds to 5.0/1023 ≈ 4.9 mV. The voltage is then converted to a gas reading in parts per million (ppm) with a linear scale factor for each gas:

$$C_{\text{CO}} = V_{\text{out}} \times S_{\text{CO}} \times k_{\text{CO}} \quad (2)$$

$$C_{\text{CH4}} = V_{\text{out}} \times S_{\text{CH4}} \times k_{\text{CH4}} \quad (3)$$

In (2) and (3), S_{CO} and S_{CH4} are the base sensitivity factors of the ZE07-CO and TGS2611 sensors, and k_{CO} and k_{CH4} are empirically determined scale constants, set to 100 and 1000, respectively. This single-factor linear mapping is a first-order approximation. An electrochemical CO sensor such as the ZE07-CO is approximately linear over its rated range [24].

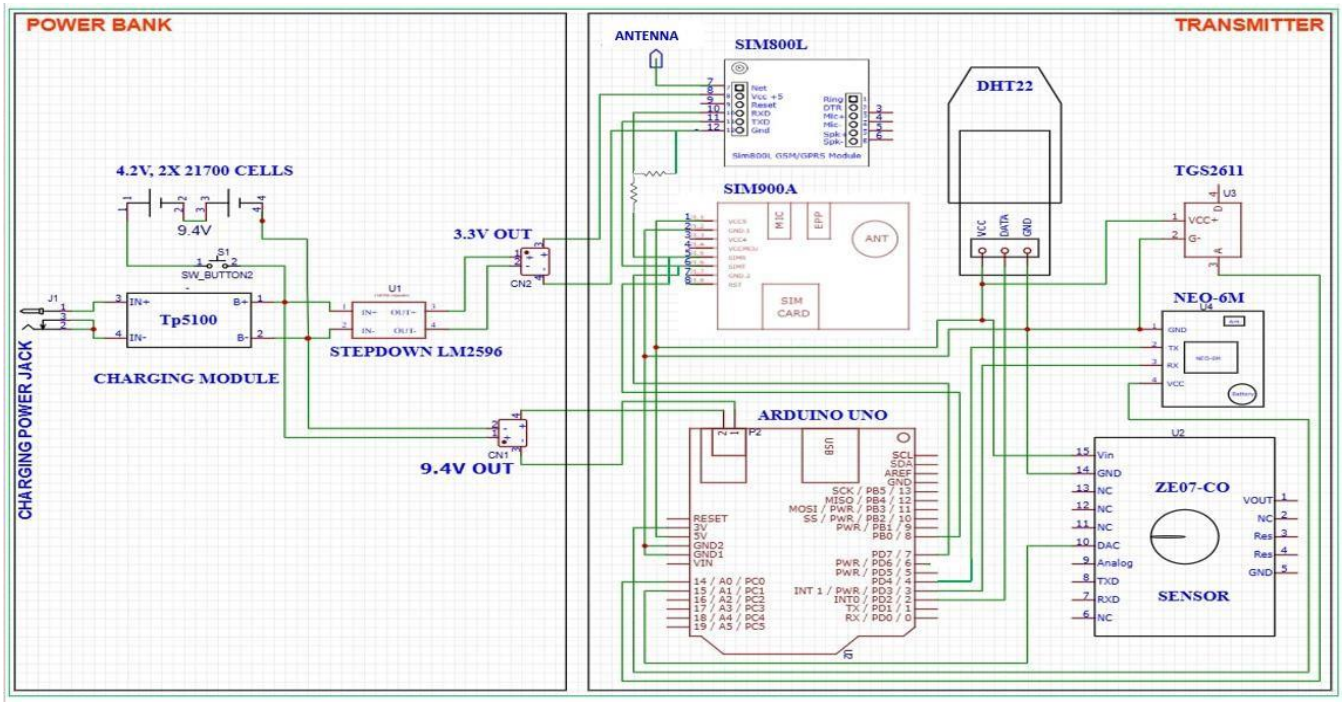


Fig. 6. Schematic configuration of the transmitter node

The TGS2611, however, is a metal-oxide semiconductor sensor whose resistance varies non-linearly with methane concentration and also depends on temperature and humidity; it additionally responds to hydrogen, ethanol and iso-butane [25]. Its typical detection range is 500-10,000 ppm of methane [25], well above the levels expected in ambient urban air. The CH_4 values reported in Section V (about 8-13 ppm) therefore lie below the specified range of the sensor and must not be read as absolute methane concentrations. They are an uncalibrated, relative response of the TGS2611 (a CH_4-equivalent index) and are used here only to compare sites and times. The CO values are likewise not calibrated against a reference analyzer.

D. Data Visualization

This section describes the live, interactive dashboard implemented to visualize the data. The dashboard is built on the Google Firebase Realtime Database [6], a cloud-hosted NoSQL (JSON) database that synchronizes data to connected client applications in real time. The real-time web dashboard shows temperature, humidity, CO and CH_4 together with the historical trend of each parameter as shown in the dashboard screenshot of Fig. 7.

E. Communication Performance

The sensor node sends one SMS per sampling interval. Each message is a short text packet of about 80 characters a shown in the sample of Fig. 4, well within the 160-character limit of a single SMS. SMS is a store-and-forward service: the delivery time depends on the carrier's message centre and on network load, and delivery is not guaranteed. In the present field test, per-message latency and packet loss were averaged at 15 s and 3% respectively, and the arrival of readings at the dashboard for each site was also used as a qualitative indication that the link worked along the route.

F. Device Fabrication

The transmitter node is organized in two layers as shown in Fig. 8. The top layer includes the microcontroller, the GSM and GPS modules, the CO and CH_4 gas sensors and the humidity-temperature sensors, while the lower layer includes the power supply unit.. The separation of layers is intended to reduce the coupling of electrical noise and electromagnetic interference generated by the power-supply stage into the sensing and communication circuits. The benefit of this separation was not quantified in this study (for example, by comparing noise levels with and without separation) and is left for future work.

To prevent PCB flexural strain and resulting damage to solder joints, all these elements are mechanically constrained within a protective cover and attached to a rigid base plate by spacers and bolts. The structure protects the node from vibration, shock, and environmental exposure and makes it suitable for mobile outdoor applications. The receiver node contains the ESP32 module, a GSM/GPRS communication module, and a DC-DC buck converter, as shown in Fig. 9. The ESP32 collects data wirelessly, while the GSM module connects the system to the cloud. The buck converter protects sensitive electronics by converting voltage levels, and it enables continuous environmental monitoring in the field.



Fig. 7. Mobile portable dashboard which displays the real time location on map of the sensor nodes, CH_4, CO, humidity levels and temp

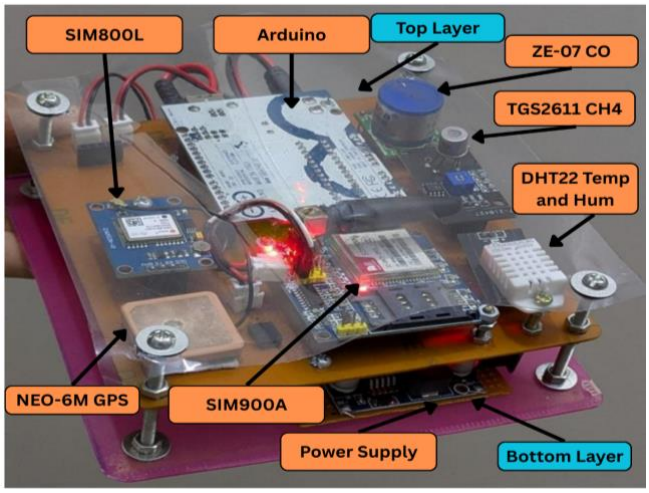


Fig. 8. The model of sensor node prepared with the controller, power supply, GSM module and GPS module, environmental sensors and also different gas sensors.

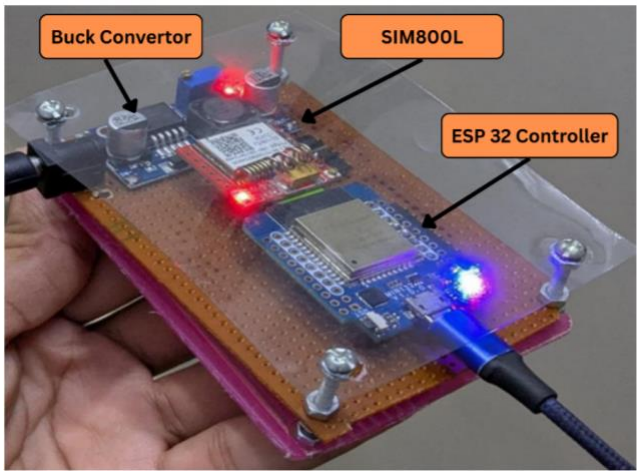


Fig. 9. Picture of the developed Receiver Node

V. Results and Discussion

In this section, we present the results acquired from experimental testing for pollution mapping between Karsaz Road and NED University Campus in urban Karachi, Pakistan (14.2 km). The experiments were conducted in the morning (06:00 AM to 06:45 AM) and at night (09:00 PM to 09:45 PM), with one drive of the route in each period, to capture the differences in environmental conditions between the two periods, which are expected to differ in traffic density.

The distance covered for the experiment was 14.2-km as

shown in Fig. 10. The area is characterized by a mixture of residential and commercial premises with moderate to high traffic density. Traffic along the route consists of cars, buses, rickshaws, and motorcycles. To characterize the pollution levels, readings were recorded at nine sites along the route (site numbers 1–9 shown in Figures 11 to 14), chosen as highly congested locations; no traffic counts or meteorological data were recorded. Temperature, humidity, CH_4 and CO concentrations were measured using a portable IoT-based monitoring system fitted with appropriate sensors. Data was uploaded on a remote repository through Firebase to visualize and analyze the pollution levels on an android mobile application in real time.

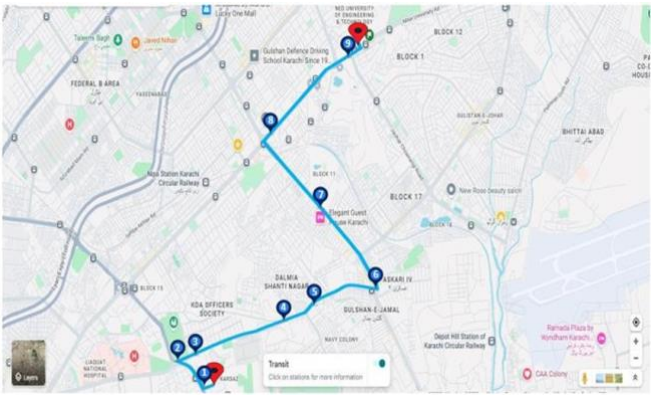


Fig. 10. Shows the sequence of air quality data collection showing the road route taken for drive testing

Figs. 11, 12, 13, and 14 compare the temperature, humidity, CO and CH_4 readings, respectively, between the morning and night runs. As seen from the figures, most parameters fluctuate between sites, with the highest temperature and pollutant readings generally observed at congested sites along the route as indicated in Fig. 10. Because no traffic counts were recorded, this association with traffic is qualitative. The findings indicate that the temperature rises during the course of a day from 29.2 to 35.3°C (difference of 6.1°C), while the humidity decreases from 22.6 to 13.4% (difference of 9.2%). In addition, CO levels increased between morning and night from 4.7 to 5.7 ppm (difference of 1.0 ppm), while levels of CH_4 decreased from 13.2 to 8.5 ppm (difference of 4.7 ppm). Table II provides a summary statistic of the parameters observed, collected for both runs and all nine sites, so the standard deviations include the morning to night difference and are not descriptions of the frequently of the measurements.

Several features of these results need careful interpretation. The morning to night differences in temperature (6.1 °C) and humidity (9.2 percentage points) are much larger than the rated uncertainty of the DHT22 (±0.5 °C and ±2% RH, at most ±5% RH) [23], so they are unlikely to be measurement noise alone. A higher temperature at 09:00 PM than at 06:00 AM is plausible, because 06:00 AM is close to the daily minimum, whereas in the night the air, roads and buildings are still releasing heat absorbed during morning (urban heat island effect), and relative humidity falls as temperature rises. However, the night humidity readings are almost identical at most sites (see Fig. 12), and as the sensor was mounted on a vehicle, enclosure self-heating, vehicle thermal environment and sensor response time may have contributed; this measurement should be verified with a reference hygrometer. CO was higher at night, consistent with continual night traffic and reduced post-sunset atmospheric dispersion, but this is untestable as traffic counts or wind/boundary layer data were not collected: CH_4 fell while CO was rising, inconsistent with a common vehicular source. This is probably due to the TGS2611: it operates below its rated range at these levels, its output is temperature and humidity dependent (which differed between the runs) and it responds to other combustible gases [25]. The CH_4 trend is therefore not interpreted as a real change in methane concentration.

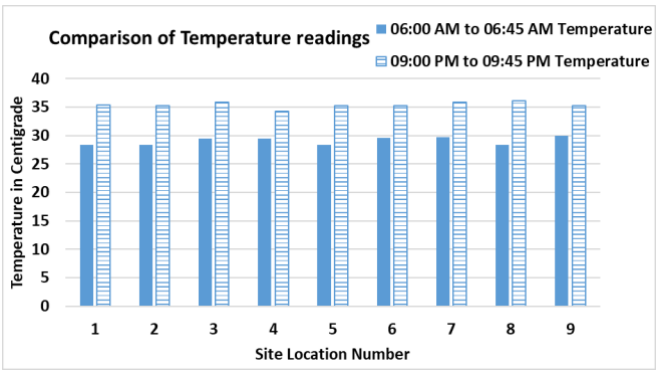


Fig. 11. Comparison of temperature data collected in the morning to the data collected at night

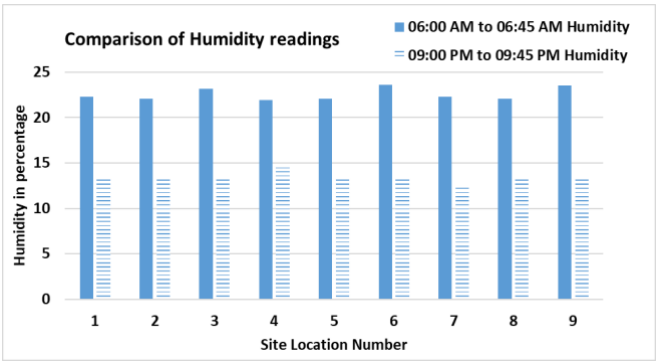


Fig. 12. Comparison of humidity data collected in the morning to the data collected at night

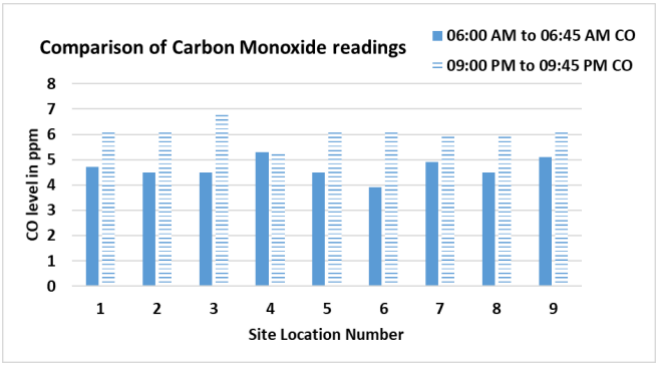


Fig. 13. Comparison of CO data collected in the morning to the data collected at night

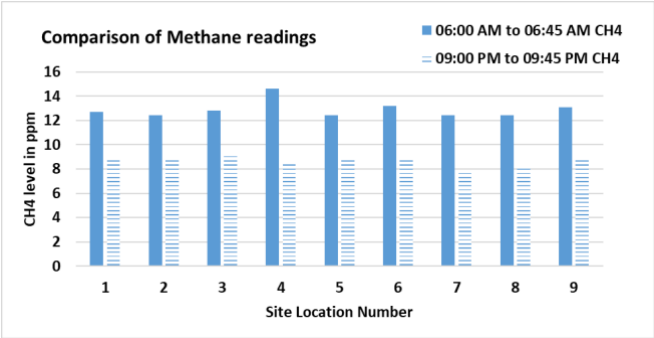
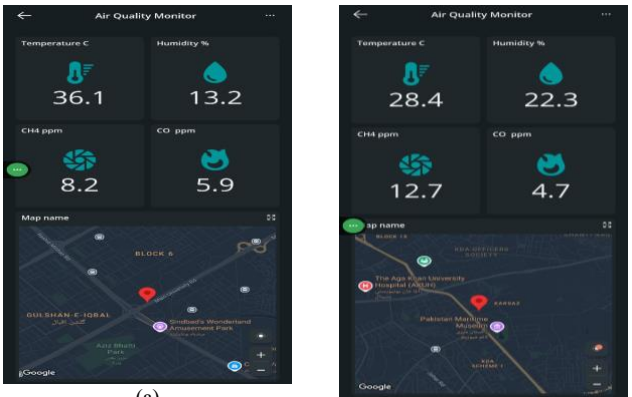


Fig. 14. Comparison of CH_4 data collected in the morning to the data collected at night

These results demonstrate the system's ability to acquire, transmit, and display in real time geo-tagged readings of temperature, humidity, CO and CH_4 along an urban route. Because no co-located reference measurements were collected, the absolute accuracy of the readings has not been established, and the results should be regarded as a proof of concept demonstration as discussed in Section VI. The android app developed for the project provides an appropriate remote access interface to the system. It offers a real-time view of the environmental conditions in terms of temperature, humidity, CO and CH_4 concentration. In addition, it allows the tracking of the system's location in real-time. This gives an indication of the pollution levels at various points along the route and allows users to monitor trends and access location-based pollution data in real time. The application is synchronized with the Firebase Realtime Database, enabling a seamless flow of data from sensors to end-users. Fig. 15 shows the comparison of the sensors' readings and GPS location display on mobile application as observed when the node was present at (a) NED University Campus and (b) Karsaz Road.

TABLE II
Mean and Standard Deviation of the Observed Air Quality Parameters

Parameter	Mean	Standard Deviation
Temperature (°C)	32.21	3.28
Humidity (%)	17.99	4.75
CO (ppm)	5.37	0.83
CH_4 (ppm)	10.74	2.28



(a) (b)

Fig. 15. Real-Time Sensor Readings and GPS Locations on two different sites (a) NED University Campus, (b) Karsaz Road, as shown in Mobile App

VI. LIMITATIONS

This study is a proof of concept of the cellular IoT based air quality monitoring system using GSM modules to transmit field data through cellular system. However, there are some limitations that must be clearly understood. First, the gas channels used fixed linear scale factors and were not calibrated against a reference analyzer. Second, cross-sensitivity and environmental effects were not compensated. The TGS2611 responds to hydrogen, ethanol and iso-butane and varies with temperature and humidity [25], the ZE07-CO shows similar dependencies [24], and mounting the node on a vehicle may add self-heating and exhaust effects. Third, the dataset is one drive per period over nine sites, with no repeated runs, traffic counts or meteorological data. The morning–night differences are therefore indicative and cannot be attributed to traffic alone. Fourth, a single mobile node limits spatial coverage, and the Electromagnetic Interference (EMI) benefit of the two-layer design has not been measured. Future work will address these through co-located calibration with temperature and humidity compensation, repeated drives with recorded traffic and weather, and a multi-node deployment.

VII. CONCLUSION

This paper presented design, implementation, and field results for a low cost cellular IoT system for real-time geo-tagged mapping of air pollution in cities. The proposed system used low cost sensors (DHT22, ZE07-CO, TGS2611, and NEO-6M GPS) for the measurement of temperature, humidity, CO, CH_4 and GPS location information. A novel approach to the architecture of the system involved a two-layer data transmission scheme, whereby the GSM module is used for data acquisition in the field, and the on-board Wi-Fi is used to post-process the acquired JSON-formatted data to the Firebase database, with timestamps provided by the NTP server. Another unique aspect of this system is a two-layer transmitter hardware design, which physically isolates the sensors from the power supply, intended to reduce EMI. The degree to which this design actually reduces interference is yet to be determined. The system was tested in the field by driving a 14.2 km circuit through heavily populated areas of Karachi, Pakistan on both a morning and night. The system was observed to function properly, and GPS-tagged values were recorded at 9 sampling points, with notable differences in the values recorded in the morning and the night. Due to the lack of calibration of the gas sensors against a reference instrument, and the single run of the circuit per day, these results should be considered a proof of concept, and the values from the CH_4 sensor in particular should be considered approximate values for the relative levels of methane in the environment. The results nevertheless indicate the potential of the system for studying dynamic urban pollution. The system is low-cost, portable and cloud-connected and can complement fixed monitoring stations. Future work will focus on co-locating the node with reference analyzers for calibration, quantifying the EMI benefit, repeating the drives to obtain statistical results, expanding the types of sensors (e.g., PM2.5, NO_2), using machine learning based calibration methods to enhance the accuracy of sensors, and building a

network of multiple nodes to monitor the spatio temporal pollution

Funding Statement

The author(s) received no specific funding for this study.

Conflicts of Interest

The authors declare no conflicts of interest to report regarding the present study.

Author Contributions

Pakeeza Noor: Methodology, Formal analysis, Investigation, Software, Visualization, Writing - Original Draft; Sundus Ali: Conceptualization, Methodology, Validation, Resources, Data Curation, Writing - Review & Editing; Irfan Ahmed: Software, Validation, Data Curation, Writing - Review & Editing; Muhammad Imran Aslam: Conceptualization, Resources, Supervision, Project administration, Writing - Review & Editing.

Institutional Review Board Statement

Not applicable.

Informed Consent Statement

Not applicable.

Data Availability Statement

The drive testing data reported in this paper is deposited in a public repository and available at the following DOI. https://doi.org/10.5281/zenodo.23302668

CONSENT FOR PUBLICATION

All authors have read and approved the final version of the manuscript and consent to its publication.

DECLARATION OF GENERATIVE AI IN SCIENTIFIC WRITING

For preparing this manuscript, the authors have only made use of generative artificial intelligence systems to enhance language proficiency, grammar, and readability.

References

[1] World Health Organization, "WHO ambient (outdoor) air pollution," 2021.

[2] R. M. Hannun and A. H. Abdul Razzaq, "Air pollution resulted from coal, oil and gas firing in thermal power plants and treatment: A review," *IOP Conf. Ser., Earth Environ. Sci.*, vol. 1002, no. 1, Art. no. 012008, 2022.

[3] M. Aleixandre and M. Gerboles, "Review of small commercial sensors for indicative monitoring of ambient gas," *Chem. Eng. Trans.*, vol. 30, pp. 169–174, 2012.

[4] H. Zou et al., "Towards occupant activity driven smart buildings via WiFi-enabled IoT devices and deep learning," *Energy Buildings*, vol. 177, pp. 12–22, 2018.

[5] K. Zheng et al., "Design and implementation of LPWA-based air quality monitoring system," *IEEE Access*, vol. 4, pp. 3238–3245, 2016.

[6] Google, "Firebase Firestore," 2025. [Online]. Available: https://firebase.google.com/docs/firestore/ (accessed Mar. 16, 2026).

[7] E. G. Snyder et al., "The changing paradigm of air pollution monitoring," *Environ. Sci. Technol.*, vol. 47, no. 20, pp. 11369–11377, 2013.

[8] A. P. Jones, "Indoor air quality and health," *Atmos. Environ.*, vol. 33, no. 28, pp. 4535–4564, 1999.

[9] P. Kumar et al., "The rise of low-cost sensing for managing air pollution in cities," *Environ. Int.*, vol. 75, pp. 199–205, 2015.

[10] A. C. Rai et al., "End-user perspective of low-cost sensors for outdoor air pollution monitoring," *Sci. Total Environ.*, vol. 607, pp. 691–705, 2017.

[11] A. Medina-Pérez, D. Sánchez-Rodríguez, and I. Alonso-González, "An internet of thing architecture based on message queuing telemetry transport protocol and Node-RED: A case study for monitoring radon gas," *Smart Cities*, vol. 4, no. 2, pp. 803–818, 2021.

[12] A. Kumar, M. Kumari, and H. Gupta, "Design and analysis of IoT based air quality monitoring system," in *Proc. Int. Conf. Power Electron. IoT Appl. Renew. Energy Control (PARC)*, 2020.

[13] D. Hercog et al., "Design and implementation of ESP32-based IoT devices," *Sensors*, vol. 23, no. 15, p. 6739, 2023.

[14] M. Cardenas-Juarez et al., "Implementation of a low-cost IoT indoor air quality monitor in dynamic public environments," in *Proc. IEEE Virtual Conf. Commun. (VCC)*, 2024.

[15] S. Ali et al., "Low cost sensor with IoT LoRaWAN connectivity and machine learning-based calibration for air pollution monitoring," *IEEE Trans. Instrum. Meas.*, vol. 70, pp. 1–11, 2021.

[16] W. A. Jabbar et al., "LoRaWAN-based IoT system implementation for long-range outdoor air quality monitoring," *Internet Things*, vol. 19, Art. no. 100540, 2022.

[17] Tanzila et al., "Prototyping LoRaWAN-based mobile air quality monitoring system for public health and safety," *Eng. Proc.*, vol. 118, no. 1, p. 20, 2025.

[18] K. M. Abubeker et al., "Internet of Things and LoRaWAN-assisted real-time indoor air quality monitoring and automation system for enhancing passenger safety," *Int. J. Low-Carbon Technol.*, vol. 20, pp. 1427–1439, 2025.

[19] R. Mumtaz et al., "Internet of things (IoT) based indoor air quality sensing and predictive analytic—A COVID-19 perspective," *Electronics*, vol. 10, no. 2, p. 184, 2021.

[20] J. Pantelic et al., "Cooking emission control with IoT sensors and connected air quality interventions for smart and healthy homes: Evaluation of effectiveness and energy consumption," *Energy Buildings*, vol. 286, Art. no. 112932, 2023.

[21] M. N. Ramadan et al., "Real-time IoT-powered AI system for monitoring and forecasting of air pollution in industrial environment," *Ecotoxicol. Environ. Saf.*, vol. 283, Art. no. 116856, 2024.

[22] M. Abdullah et al., "Development of cellular IoT-based, portable outdoor air quality monitoring system for pollution mapping," *Eng. Proc.*, vol. 118, no. 1, p. 30, 2025.

[23] Mouser Electronics, "DHT22 sensor datasheet," 2025. [Online]. Available: https://www.mouser.com/datasheet/2/737/dht-932870.pdf (accessed Oct. 17, 2026).

[24] Winsen, "ZE-07 carbon monoxide sensor," 2026. [Online]. Available: https://www.winsen-sensor.com/d/files/PDF/Gas%20Sensor%20Module/CO%20Detection%20Module/ZE07%20CO%20Module%201.3V.pdf (accessed Mar. 16, 2026).

[25] Figaro, "TGS-2611 sensor datasheet." [Online]. Available: https://www.figarosensor.com/product/docs/TGS%202611C00(1013).pdf (accessed Mar. 16, 2026).

[26] Espressif Systems, "ESP32." [Online]. Available: https://www.espressif.com/en/products/socs/esp32 (accessed May 2, 2025).

[27] SIMCom, "SIM800L GSM module datasheet," 2025.

[28] SIMCom, "SIM900A GSM module hardware design guide," 2025.

[29] u-blox, "NEO-6M GPS module datasheet," 2025. [Online]. Available: https://content.u-blox.com/sites/default/files/products/documents/NEO-6_DataSheet_%28GPS.G6-HW-09005%29.pdf (accessed Mar. 3, 2026).